

# Generation of Giant Unilamellar Liposomes Containing Biomacromolecules at Physiological Intracellular Concentrations using Hypertonic Conditions

Kei Fujiwara<sup>\*,†</sup> and Miho Yanagisawa<sup>\*,‡</sup>

<sup>†</sup>Department of Bioengineering and Robotics, Graduate School of Engineering, Tohoku University, 6-6-01 Aramaki-aza Aoba, Aoba-ku, Sendai 980-8579, Japan

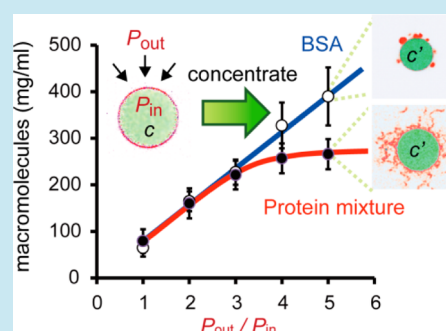
<sup>‡</sup>Department of Physics, Graduate School of Sciences, Kyushu University, 6-10-1 Hakozaki, Higashi-ku, Fukuoka 812-8581, Japan

## S Supporting Information

**ABSTRACT:** Artificial cells, particularly cell-sized liposomes, serve as tools to improve our understanding of the physiological conditions of living cells. However, such artificial cells typically contain a more dilute solution of biomacromolecules than that found in living cells ( $300 \text{ mg mL}^{-1}$ ). Here, we reconstituted the intracellular biomacromolecular conditions in liposomes using hyperosmotic pressure. Liposomes encapsulating  $80 \text{ mg mL}^{-1}$  of macromolecules of BSA or a protein mixture extracted from *Escherichia coli* were immersed in hypertonic sucrose. The concentration of macromolecules in BSA-containing liposomes was increased in proportion to the initial osmotic pressure ratio between internal and external media. On the other hand, the concentration of the protein mixture in liposomes could be saturated to reach the physiological concentration of macromolecules in cells. Furthermore, membrane transformation

after the hypertonic treatment differed between BSA- and protein mixture-containing liposomes. These results strongly suggested that the crowded environment in cells is different from that found in typical single-component systems.

**KEYWORDS:** phospholipid vesicle, molecular crowding, origin of life, shape deformation, artificial cells



Living cells contain high concentrations ( $>300 \text{ mg mL}^{-1}$ ) of cytoplasmic macromolecules inside biomembranes.<sup>1,2</sup> This environment affects the kinetics of biochemical reactions (such as catalytic reactions, binding reactions, and protein folding) and is referred to as the macromolecular crowding effect.<sup>2–6</sup> Moreover, confinement within biomembranes also affects biochemical reactions in cells.<sup>7–12</sup> Thus, artificial cells entrapping high concentrations of macromolecules should be constructed in order to facilitate a better understanding of the cytoplasmic environment based on physicochemical aspects.

To achieve this, researchers have prepared high-concentration macromolecule mixtures, similar to those observed in cells. Recently, we extracted a functional protein mixture from *Escherichia coli* without adding buffers or salts (hereafter called an additive-free cell extract [AFCE]).<sup>13</sup> In that study, the AFCE was concentrated by gradual evaporation in a desiccator to reach a physiological intracellular macromolecule concentration. However, this process took nearly 4 h, and the condensed AFCE was too viscous to be used in further analyses.

The liposomal membrane allows small molecules to permeate, such as water ( $\sim 10^{-2} \text{ cm s}^{-1}$ ) and glycerol ( $\sim 10^{-6} \text{ cm s}^{-1}$ ); however, macromolecules with higher molecular weights of  $\gg 100 \text{ Da}$  or charged molecules generally cannot diffuse through the liposomal membrane.<sup>14</sup> When the osmotic pressure of the outer media is higher than that of the inner media ( $P_{\text{out}}/P_{\text{in}} \geq 1$ ), the efflux of small molecules exceeds the

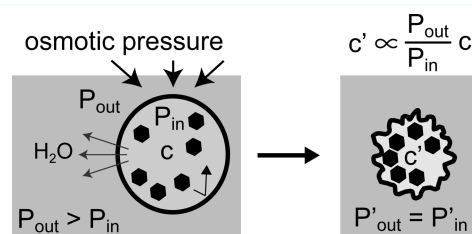


**Figure 1.** Strategy for concentrating macromolecules in a liposome under hypertonic conditions. The initial concentration of macromolecules in liposomes ( $c$ ) increases in proportion to the initial osmotic pressure ratio between the outer and inner media ( $P_{\text{out}}/P_{\text{in}} > 1$ ) and achieves a final value ( $c'$ ) at an isotonic condition ( $P'_{\text{out}} = P'_{\text{in}}$ ).

influx and reduces the inner volume of the liposome, as illustrated in Figure 1. In contrast, the surface area of a liposome remains constant. Therefore, the liposome deforms its shape using the larger area/volume ratio. Accordingly, the concentration of inner molecules ( $c$ ) increases with time and achieves a final value ( $c'$ ) in proportion to the initial osmotic pressure ratio ( $P_{\text{out}}/P_{\text{in}}$ ) when the osmotic pressures of the inner and outer media are equivalent ( $P'_{\text{out}} = P'_{\text{in}}$ ). Consequently, macromolecules inside liposomes should be

Received: November 27, 2013

Published: February 4, 2014

concentrated when the outer media are maintained at a higher osmotic pressure.

Here, we report the development of a new concentration method that uses the semipermeable properties of the liposomal membrane. We showed that macromolecules could be condensed in liposomes at hyperosmotic pressures. This method enabled us to make liposomes containing physiological concentrations of biomacromolecules, and these liposomes are expected to be useful for improving our understanding of the critical differences between living matter and material.

Liposomes were prepared using the modified droplet-transfer method described in the Methods section. The concentration of macromolecules inside liposomes prepared using our method was maintained at a constant level during the experimental period (Supporting Information, Figure S1). The initial solution used for encapsulation in liposomes was 80 mg mL<sup>-1</sup> of AFCE or BSA. AFCE prepared from *E. coli* contained 80 mg mL<sup>-1</sup> of macromolecules (55 mg mL<sup>-1</sup> of proteins and 25 mg mL<sup>-1</sup> of nucleotides) and had an osmotic pressure of 70 mosM. Small metabolites extracted from cells mainly contributed to the osmotic pressure of the AFCE being 70 mosM, and biomacromolecules (mainly proteins and RNAs) contributed only a few mosM. The encapsulation of these biomacromolecules at lower concentrations decreased the generation efficiency of liposomes, and this effect may be related to the stability of droplets passing through the oil/water interface.<sup>15</sup> Green fluorescent protein (GFP) was used to estimate the macromolecular concentration. To prepare the AFCE, we used cells that expressed relatively low levels of GFP *in vivo*, facilitated by leaky expression of the *tac* promoter.<sup>16</sup> Analysis of fluorescence intensity showed that the AFCE contained 2.2 μM GFP.<sup>16</sup> BSA was dissolved in 70 mM sucrose with 3.1 μM GFP. The outer solution was 70 mM glucose with an osmotic pressure equivalent to that of the inner solution. To concentrate these, we added sucrose as an osmolyte at final concentrations ranging from 70 to 350 mM.

We first used a lipid mixture of DOPE and DOPC (2:1) to prepare liposomes. Use of this lipid composition allowed us to obtain relatively large liposomes, although clusters of liposomes were still observed. The diameters of liposomes ranged from 10 to 100 μm. Macromolecules encapsulated in liposomes were concentrated by immersion in sucrose such that the osmotic pressure of the outer media was higher than that of the inner media ( $P_{\text{out}} > P_{\text{in}} = 70$  mosM; Figure 2A). The volume of liposomes ( $v$ ) gradually decreased after the addition of sucrose. Figure 2B shows an example of liposomes at  $P_{\text{out}} = 285$  mosM, where the largest liposome at the center (arrow) shrank from 48 to 35 μm in diameter 360 s after the addition of sucrose. Accordingly, we observed an increase in the fluorescence intensity of entrapped GFP per unit volume ( $I$ ), which indicates the concentration of macromolecules in the liposome.

The correlation between the values of  $I$  and  $v$  was analyzed by tracking identical liposomes. The volumes of shrunk liposomes were estimated from the average diameters. The change in volume is expressed as the volume ratio before and after condensation ( $v_0/v \geq 1$ ). Under hypertonic conditions at  $P_{\text{out}} = 285$  mosM, the changes in volume ratio  $v_0/v$  were tracked by taking time-lapse images of five different liposomes (Figure 3, colored lines). Changes in the volume ratio normalized to the initial volume ( $v_0/v$ ) after the hypertonic treatment were independent of the initial liposome size (Supporting Information, Figure S2). The average of the fitted plots showed that changes in the liposome volume plateaued at

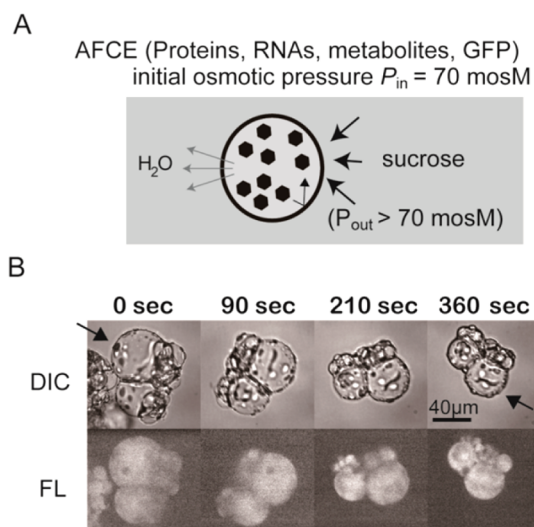


**Figure 2.** Kinetics of concentrating macromolecules in a liposome. (A) Schematic illustration of the experiment performed in the AFCE system. (B) Time-lapse images of liposomes after sucrose addition ( $P_{\text{out}} = 285$  mosM,  $P_{\text{in}} = 70$  mosM). Representative differential interference contrast (DIC) and GFP fluorescence images inside liposomes (FL) are shown.

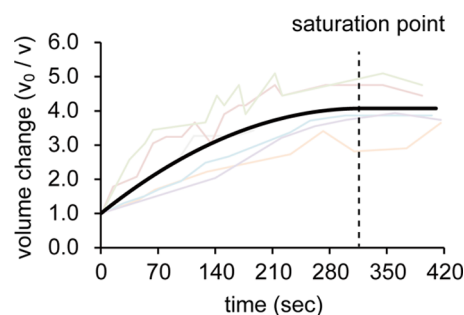


**Figure 3.** Changes in the volume ratio normalized to the initial value ( $v_0/v$ ) plotted against time after the addition of sucrose. Colored and black lines indicate data from five liposomes and the average data of their fitted lines, respectively. The condensation time until the saturation point was about 320 s. The initial diameters of the liposomes were 27, 28, 33, 50, and 86 μm.

320 s (Figure 3, black line). We called this time the “condensation time”. The final value of  $v_0/v$  was approximately 4. In addition, GFP concentrations inside liposomes increased in proportion to an increase in  $v_0/v$  (Supporting Information, Figure S3). These data showed that GFP did not exit the membrane, but instead became concentrated inside the liposome.

The final concentration ( $c'$ ) was expected to increase in proportion to the initial osmotic pressure ratio of the outer and inner media ( $P_{\text{out}}/P_{\text{in}}$ ). To confirm that the experimental conditions were consistent with this theory, we examined the relationship between the values of  $c'$  and  $P_{\text{out}}/P_{\text{in}}$ . In this case, we used liposomes made from eggPC lipids to obtain isolated liposomes. Sucrose solutions at different values of  $P_{\text{out}}/P_{\text{in}}$  were mixed with the solution of liposomes containing AFCE or BSA. Although  $P_{\text{out}}/P_{\text{in}} = 5.0$  was not the maximum possible value that could be achieved in this experiment, the range of  $P_{\text{out}}/P_{\text{in}}$  was set from 1.0 to 5.0 to analyze biomacromolecule concentrations within the physiological range (300 mg mL<sup>-1</sup>).<sup>1</sup> The inner media contained a certain amount of

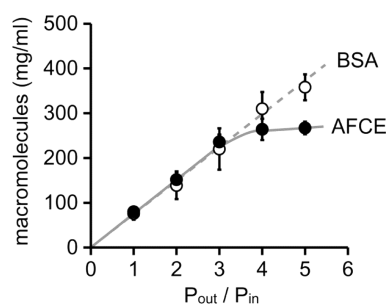


**Figure 4.** Macromolecule concentrations in liposomes under various hypertonic conditions. The final concentration of macromolecules concentrated inside a liposome, estimated from the GFP intensity, was plotted against the initial osmotic pressure ratio ( $P_{out}/P_{in}$ ). Error bars indicate the standard errors ( $n = 18-43$ ). The dashed line indicates the theoretical concentration, and the black line is fitted to the AFCE data.

GFP, which was assumed to be proportional to the macromolecule concentration in the liposome. GFP concentrations were determined after 1 h, which was much longer than the condensation time (Supporting Information, Figure S4). Final GFP concentrations inside liposomes were uniform across all examined liposome sizes (Supporting Information, Figure S5). In the case of BSA, the value of  $c'$  was linearly related to the value of  $P_{out}/P_{in}$ , indicating that the condensation of macromolecules proceeded based on the theory (Figure 4). On the other hand, the value of  $c'$  for the AFCE system exhibited characteristics of a saturation curve. The fitting line suggested that the maximum concentration of macromolecules at  $P_{out}/P_{in} > 3$  was near  $300 \text{ mg mL}^{-1}$ , which is very similar to the concentration of macromolecules found in living cells.<sup>1</sup>

The osmotic pressure of the biomacromolecule solution increases nonlinearly at higher concentrations, and changes in pH values and ionic strengths affect the degree of increase.<sup>17,18</sup> Minton explained this relationship using an effective hard particle model.<sup>19</sup> Our BSA solutions contained 70 mM sucrose and a very low concentration of salts ( $<1 \text{ mM}$ ) derived from the GFP solution; the pH was 7.0. The linear relationship of the BSA liposomes with  $P_{out}/P_{in}$  suggested that the contribution of BSA to the osmotic pressure of the solution was smaller than that of sucrose under these experimental conditions. The AFCE contained various small molecules and various biomacromolecules. Therefore, we assumed that the changes in osmotic pressure and/or the high viscosity of the AFCE mentioned above would determine the appearance of the saturation point of the AFCE in a complex manner. Further studies are needed to reveal why the condensation of the AFCE stops at the saturation point.

Fluorescence images of lipid membranes (Figure 5) demonstrated that a higher  $P_{out}/P_{in}$  yielded more dramatic shape deformations in liposomes with increasing area/volume ratios. The types shape deformations for the liposomes encapsulating BSA and AFCE were different from each other. In the case of liposomes containing BSA, redundant membranes after hypertonic treatment formed several buds to the outside. On the other hand, tubular formation of the redundant membrane was observed in liposomes containing  $\sim 300 \text{ mg mL}^{-1}$  of AFCE.

External osmotic pressure deforms the shape of liposomes without macromolecules.<sup>20-22</sup> Such liposomes use their redundant membranes to transform their shapes, thereby minimizing the bending energy of the membranes.<sup>23-25</sup> The

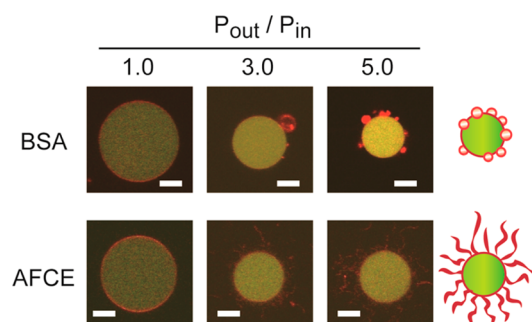


**Figure 5.** Distinct deformation patterns of artificial cells encapsulating a single component (BSA) and multiple components (AFCE). Fluorescence images demonstrated the presence of membrane deformation in liposomes (red) encapsulating macromolecules and GFP (green). The schematic images at the right edge show the typical types of liposome deformation patterns observed for BSA- and AFCE-containing liposomes, *i.e.*, budding and tubulation of membranes. Scaled bars indicate  $5 \mu\text{m}$ .

bending energy of a liposome membrane increases with  $R^{-2}$ , where  $R$  is the radius. In contrast, our liposomes, which entrapped high concentrations of macromolecules, showed completely different deformation patterns according to the contents inside the liposome. Previous studies have indicated that BSA uniformly diffuses inside giant unilamellar liposomes,<sup>9,26</sup> and therefore, the budding deformation pattern seems to occur irrespective of the specific characteristics of BSA. Indeed, BSA-containing liposomes formed vesicles using the redundant membrane, similar to the budding observed in phase-separating liposomes.<sup>25</sup> On the other hand, AFCE-containing liposomes shrunk their spherical regions and showed tubules derived from the redundant membranes (Figure 5). This difference may have arisen from the limitations of the internal space and interactions between the lipid membrane and the viscoelastic inner solution. The concentrated AFCE was estimated to be much more viscous than the concentrated BSA because thinner, tubular liposomes have much higher bending energies than spherical liposomes and because the condensation was stopped at a certain concentration of AFCE, unlike for BSA (Figure 4). Further studies are required to determine how shape deformation of liposomes depends on the viscoelastic properties of the entrapped macromolecules as well as the physicochemical properties of the liposomes. To the best of our knowledge, this is the first report describing the shrinking behaviors of giant liposomes containing high concentrations of biomacromolecules.

In this study, we achieved reconstitution of intracellular macromolecular concentrations in liposomes using hypertonic conditions, reaching concentrations greater than  $300 \text{ mg mL}^{-1}$ . We found that the saturation points of the concentrations and membrane transformations after the treatment were significantly different between liposomes containing a single component protein (BSA) and those containing the protein mixture (AFCE). These results clearly indicated that macromolecular crowding of multiple components in cells was distinct from the environment within single-component systems. Hence, the present findings provide important insights into our understanding of membrane deformation and homeostasis of living cells from physical and biological viewpoints.

## METHODS

**Materials.** EggPC, 1,2-dioleoyl-sn-glycero-3-phosphocholine (DOPC), and 1,2-dioleoyl-sn-glycero-3-phosphoethanolamine (DOPE) were purchased from Wako Chemicals (Osaka, Japan). All lipids were used without further purification, and 10 mM of each lipid was stored in chloroform at  $-20\text{ }^{\circ}\text{C}$ . A light and viscous mineral oil (0.84 g/L at  $15\text{ }^{\circ}\text{C}$ , Nacalai Tesque, Kyoto, Japan, product code: 23306–84) was used to prepare liposomes using the droplet-transfer method mentioned below. BSA was purchased from Sigma-Aldrich, Japan (Kyoto, Japan).

**Preparation of the AFCE.** The AFCE was prepared using previously published protocols, with slight modifications.<sup>13</sup> *E. coli* BL21 (DE3) cells harboring pTD-sfGFP were grown to 1.0 OD<sub>600</sub> at  $37\text{ }^{\circ}\text{C}$  in LB medium, harvested, suspended in 20% w/w sucrose in 20 mM Tris-HCl (pH 8.0), and incubated on ice for 10 min. Cells were then washed with 4 volumes of double-distilled water (DDW), suspended in DDW, incubated on ice for 10 min, and then washed again with DDW. After centrifugation, cell pellets were stored for 1 day at  $-80\text{ }^{\circ}\text{C}$ , and the frozen cells were disrupted using a S4000 tip sonicator (MISONIX, Inc., Farmingdale, NY, USA) at 20 W for 15 min on ice. The disrupted cells were centrifuged at 30000g for 1 h, and the soluble fractions were designated as the AFCE. Protein concentrations of S30 fractions were estimated using the Bradford assay (Wako Chemicals), with BSA as a standard. The total concentration of free molecules in the S30 preparation was estimated from the osmotic pressure determined using a Vapro 5520KCE osmometer (Wescor Inc., Logan, UT, USA). To estimate the levels of GFP, the cell extracts were encapsulated in Water/Oil (W/O) droplets, and the concentrations were determined using confocal microscopy with purified GFP (prepared in our laboratory using Histidine-tagged and Ni-NTA agarose<sup>13</sup>) as a control.

**Liposome Preparation and Condensation of Macromolecules in Liposomes.** Liposomes were prepared using a modified droplet-transfer method.<sup>27–29</sup> Dry lipid films of DOPE, DOPC, or eggPC (500 nmol) were prepared on the bottom of a glass tube. To dye lipids, rhodamine-DHPE (1/200 of the total lipid amount) was added to the lipids before drying. These lipids were dissolved in mineral oil to 1 mM by ultrasonication for 90 min with a 90-W bath sonicator (Branson, Danbury, CT). DOPE oil and DOPC oil solutions were mixed 2:1 (v/v) using a vortex mixer before use. To prepare W/O droplets, 1  $\mu\text{L}$  of the AFCE was spotted on 40  $\mu\text{L}$  of a lipid-in-oil solution and was dispersed by tapping. The droplet solution was spotted on isotonic 70 mM glucose and then centrifuged at  $\sim 5000\text{g}$  for 70 s. The water phases, which contained liposomes, were collected from the bottom of the tubes. The resulting liposomes were diluted with equivalent volumes of sucrose (70–630 mM). Over 95% of liposomes survived the osmotic treatment, unlike small unilamellar liposomes.<sup>30,31</sup> After gentle mixing, samples were examined with a confocal microscope.

**Quantification of GFP Concentration.** The fluorescence intensities of GFP in liposomes were observed using a confocal laser-scanning microscope (AxioVert S100, Carl Zeiss, Jena, Germany or Olympus FV1200). The pinhole size was fixed at 3  $\mu\text{m}$ . The fluorescence intensity per area inside the liposomes, which was proportional to the GFP concentration in liposomes, was determined using ImageJ software.<sup>12</sup> Only fluorescence intensity per area around the center of liposomes was determined. The value was normalized to that of liposomes

under isotonic conditions (70 mM sucrose). Control data were analyzed using W/O droplets containing a known concentration of purified GFP in the absence of evaporation of the inner media.

## ASSOCIATED CONTENT

### Supporting Information

The relation between volume reduction of liposomes and fluorescent signals of GFP inside, and typical images after hypertonic treatment. This material is available free of charge via the Internet at <http://pubs.acs.org>.

## AUTHOR INFORMATION

### Corresponding Authors

\*E-mail: [fujiiwara@mollbot.mech.tohoku.ac.jp](mailto:fujiiwara@mollbot.mech.tohoku.ac.jp).

\*E-mail: [yanagisawa@phys.kyushu-u.ac.jp](mailto:yanagisawa@phys.kyushu-u.ac.jp).

### Notes

The authors declare no competing financial interest.

## ACKNOWLEDGMENTS

We thank Prof. Si. M. Nomura (Tohoku University, Japan) and Prof. D. Mizuno (Kyushu University, Japan) for valuable comments. This work was supported by a JSPS KAKENHI Grant (No. 23.3718, No. 23840031, and No. 24740292), the Kyushu University Interdisciplinary Programs in Education and Projects in Research Development, and a Shiseido Female Researcher Science Grant.

## ABBREVIATIONS

GFP, green fluorescent protein; BSA, bovine serum albumin; AFCE, additive-free cell extract; OD, optical density; DDW, double distilled water

## REFERENCES

- (1) Zimmerman, S. B., and Trach, S. O. (1991) Estimation of macromolecule concentrations and excluded volume effects for the cytoplasm of *Escherichia coli*. *J. Mol. Biol.* 222, 599–620.
- (2) Ellis, R. J. (2001) Macromolecular crowding: an important but neglected aspect of the intracellular environment. *Curr. Opin. Struct. Biol.* 11, 114–119.
- (3) Ellis, R. J. (2001) Macromolecular crowding: obvious but underappreciated. *Trends Biochem. Sci.* 26, 597–604.
- (4) Ellis, R. J., and Minton, A. P. (2003) Cell biology: join the crowd. *Nature* 425, 27–28.
- (5) Minton, A. P. (2006) How can biochemical reactions within cells differ from those in test tubes? *J. Cell Sci.* 119, 2863–2869.
- (6) Miyoshi, D., and Sugimoto, N. (2008) Molecular crowding effects on structure and stability of DNA. *Biochimie* 90, 1040–1051.
- (7) Hamada, T., and Yoshikawa, K. (2012) Cell-sized liposomes and droplets: Real-world modeling of living cells. *Materials* 5, 2292–2305.
- (8) Nomura, S. M., Tsumoto, K., Hamada, T., Akiyoshi, K., Nakatani, Y., and Yoshikawa, K. (2003) Gene expression within cell-sized lipid vesicles. *ChemBioChem* 4, 1172–1175.
- (9) Noireaux, V., and Libchaber, A. (2004) A vesicle bioreactor as a step toward an artificial cell assembly. *Proc. Natl. Acad. Sci. U. S. A.* 101, 17669–17674.
- (10) Ishikawa, K., Sato, K., Shima, Y., Urabe, I., and Yomo, T. (2004) Expression of a cascading genetic network within liposomes. *FEBS Lett.* 576, 387–390.
- (11) Fiordemondo, D., and Stano, P. (2007) Lecithin-based water-in-oil compartments as dividing bioreactors. *ChemBioChem* 8, 1965–1973.
- (12) Kato, A., Yanagisawa, M., Sato, Y. T., Fujiwara, K., and Yoshikawa, K. (2012) Cell-Sized confinement in microspheres accelerates the reaction of gene expression. *Sci. Rep.* 2, 283.

- (13) Fujiwara, K., and Nomura, S. M. (2013) Condensation of an additive-free cell extract to mimic the conditions of live cells. *PLoS One* 8, e54155.
- (14) Paula, S., Volkov, A. G., Van Hoek, A. N., Haines, T. H., and Deamer, D. W. (1996) Permeation of protons, potassium ions, and small polar molecules through phospholipid bilayers as a function of membrane thickness. *Biophys. J.* 70, 339–348.
- (15) Ito, H., Yamanaka, T., Kato, S., Hamada, T., Takagi, M., Ichikawa, M., and Yoshikawa, K. (2013) Dynamical formation of lipid bilayer vesicles from lipid-coated droplets across a planar monolayer at an oil/water interface. *Soft Matter* 9, 9539–9547.
- (16) Fujiwara, K., and Taguchi, H. (2007) Filamentous morphology in GroE-depleted *Escherichia coli* induced by impaired folding of FtsE. *J. Bacteriol.* 189, 5860–5866.
- (17) Vilker, V. L., Colton, C. K., and Smith, K. A. (1981) The osmotic pressure of concentrated protein solutions: Effect of concentration and pH in saline solutions of bovine serum albumin. *J. Colloid Interface Sci.* 79, 548–566.
- (18) Fane, A. G., Fell, C. J. D., and Suki, A. (1983) The effect of pH and ionic environment on the ultrafiltration of protein solutions with retentive membranes. *J. Membr. Sci.* 16, 195–210.
- (19) Minton, A. P. (2008) Effective hard particle model for the osmotic pressure of highly concentrated binary protein solutions. *Biophys. J.* 94, L57–59.
- (20) Reeves, J. P., and Dowben, R. M. (1970) Water permeability of phospholipid vesicles. *J. Membr. Biol.* 3, 123–.
- (21) Boroske, E., Elwenspoek, M., and Helfrich, W. (1981) Osmotic shrinkage of giant egg-lecithin vesicles. *Biophys. J.* 34, 95–109.
- (22) Ohno, M., Hamada, T., Takiguchi, K., and Homma, M. (2009) Dynamic behavior of giant liposomes at desired osmotic pressures. *Langmuir* 25, 11680–11685.
- (23) Menager, C., and Cabuil, V. (2002) Reversible shrinkage of giant magnetoliposomes under an osmotic stress. *J. Phys. Chem. B* 106, 7913–7918.
- (24) Bernard, A. L., Guedeau-Boudeville, M. A., Jullien, L., and di Meglio, J. M. (2002) Raspberry vesicles. *Biochim. Biophys. Acta* 1567, 1–5.
- (25) Yanagisawa, M., Imai, M., and Taniguchi, T. (2008) Shape deformation of ternary vesicles coupled with phase separation. *Phys. Rev. Lett.* 100, 148102.
- (26) Terasawa, H., Nishimura, K., Suzuki, H., Matsuura, T., and Yomo, T. (2012) Coupling of the fusion and budding of giant phospholipid vesicles containing macromolecules. *Proc. Natl. Acad. Sci. U. S. A.* 109, 5942–5947.
- (27) Pautot, S., Frisken, B. J., and Weitz, D. A. (2003) Engineering asymmetric vesicles. *Proc. Natl. Acad. Sci. U. S. A.* 100, 10718–10721.
- (28) Abkarian, M., Loiseau, E., and Massiera, G. (2011) Continuous droplet interface crossing encapsulation (cDICE) for high throughput monodisperse vesicle design. *Soft Matter* 7, 4610–4614.
- (29) Yanagisawa, M., Iwamoto, M., Kato, A., Yoshikawa, K., and Oiki, S. (2011) Oriented reconstitution of a membrane protein in a giant unilamellar vesicle: experimental verification with the potassium channel KcsA. *J. Am. Chem. Soc.* 133, 11774–11779.
- (30) Ohki, S. (1984) Effects of divalent cations, temperature, osmotic pressure gradient, and vesicle curvature on phosphatidylserine vesicle fusion. *J. Membr. Biol.* 77, 265–275.
- (31) Stevens, M. J., Hoh, J. H., and Woolf, T. B. (2003) Insights into the molecular mechanism of membrane fusion from simulation: evidence for the association of splayed tails. *Phys. Rev. Lett.* 91, 188102.